

CERN-EP-2017-342  
22 December 2017

## Search for magnetic monopoles with the MoEDAL forward trapping detector in $2.11 \text{ fb}^{-1}$ of 13 TeV proton-proton collisions at the LHC

B. Acharya,<sup>1,2</sup> J. Alexandre,<sup>1</sup> S. Baines,<sup>1</sup> P. Benes,<sup>3</sup> B. Bergmann,<sup>3</sup> J. Bernabéu,<sup>4</sup>  
A. Bevan,<sup>5</sup> H. Branzas,<sup>6</sup> M. Campbell,<sup>7</sup> L. Caramete,<sup>6</sup> S. Cecchini,<sup>8</sup> M. de Montigny,<sup>9</sup>  
A. De Roeck,<sup>7</sup> J. R. Ellis,<sup>1,10</sup> M. Fairbairn,<sup>1</sup> D. Felea,<sup>6</sup> M. Frank,<sup>11</sup> D. Frekers,<sup>12</sup> C. Garcia,<sup>4</sup>  
J. Hays,<sup>5</sup> A. M. Hirt,<sup>13</sup> J. Janecek,<sup>3</sup> D.-W. Kim,<sup>14</sup> K. Kinoshita,<sup>15</sup> A. Korzenev,<sup>16</sup>  
D. H. Lacarrère,<sup>7</sup> S. C. Lee,<sup>14</sup> C. Leroy,<sup>17</sup> A. Lioni,<sup>16</sup> J. Mamuzic,<sup>4</sup> A. Margiotta,<sup>18</sup> N. Mauri,<sup>8</sup>  
N. E. Mavromatos,<sup>1</sup> P. Mermod,<sup>19,\*</sup> V. A. Mitsou,<sup>4</sup> R. Orava,<sup>20</sup> I. Ostrovskiy,<sup>21</sup> B. Parker,<sup>22</sup>  
L. Pasqualini,<sup>18</sup> L. Patrizii,<sup>8</sup> G. E. Pávālas,<sup>6</sup> J. L. Pinfold,<sup>9</sup> V. Popa,<sup>6</sup> M. Pozzato,<sup>8</sup> S. Pospisil,<sup>3</sup>  
A. Rajantie,<sup>23</sup> R. Ruiz de Austri,<sup>4</sup> Z. Sahnoun,<sup>8,24</sup> M. Sakellariadou,<sup>1</sup> A. Santra,<sup>4</sup>  
S. Sarkar,<sup>1</sup> G. Semenoff,<sup>25</sup> A. Shaa,<sup>26</sup> G. Sirri,<sup>8</sup> K. Sliwa,<sup>27</sup> R. Soluk,<sup>9</sup> M. Spurio,<sup>18</sup>  
Y. N. Srivastava,<sup>28</sup> M. Suk,<sup>3</sup> J. Swain,<sup>28</sup> M. Tenti,<sup>29</sup> V. Togo,<sup>8</sup> J. A. Tuszyński,<sup>9</sup> V. Vento,<sup>4</sup>  
O. Vives,<sup>4</sup> Z. Vykydal,<sup>3</sup> A. Widom,<sup>28</sup> G. Willems,<sup>12</sup> J. H. Yoon,<sup>30</sup> and I. S. Zgura<sup>6</sup>

(THE MoEDAL COLLABORATION)

<sup>1</sup>*Theoretical Particle Physics & Cosmology Group,  
Physics Dept., King's College London, UK*

<sup>2</sup>*International Centre for Theoretical Physics, Trieste, Italy*

<sup>3</sup>*IEAP, Czech Technical University in Prague, Czech Republic*

<sup>4</sup>*IFIC, Universitat de València - CSIC, Valencia, Spain*

<sup>5</sup>*School of Physics and Astronomy, Queen Mary University of London, UK*

<sup>6</sup>*Institute of Space Science, Bucharest - Măgurele, Romania*

<sup>7</sup>*Experimental Physics Department, CERN, Geneva, Switzerland*

<sup>8</sup>*INFN, Section of Bologna, Bologna, Italy*

<sup>9</sup>*Physics Department, University of Alberta, Edmonton, Alberta, Canada*

<sup>10</sup>*National Institute of Chemical Physics & Biophysics, Rūvala 10, 10143 Tallinn,  
Estonia and Theoretical Physics Department, CERN, Geneva, Switzerland*

<sup>11</sup>*Department of Physics, Concordia University, Montréal, Québec, Canada*

<sup>12</sup>*Physics Department, University of Muenster, Muenster, Germany*

<sup>13</sup>*Department of Earth Sciences, Swiss Federal Institute  
of Technology, Zurich, Switzerland – Associate member*

<sup>14</sup>*Physics Department, Gangneung-Wonju National University, Gangneung, Republic of Korea*

<sup>15</sup>*Physics Department, University of Cincinnati, Cincinnati, Ohio, USA*

<sup>16</sup>*Section de Physique, Université de Genève, Geneva, Switzerland*

<sup>17</sup>*Département de physique, Université de Montréal, Québec, Canada*

<sup>18</sup>*INFN, Section of Bologna & Department of Physics & Astronomy, University of Bologna, Italy*

<sup>19</sup>*Section de Physique, Faculté des Sciences,  
Université de Genève, Geneva, Switzerland*

<sup>20</sup>*Physics Department, University of Helsinki, Helsinki, Finland*

<sup>21</sup>*Department of Physics and Astronomy,  
University of Alabama, Tuscaloosa, Alabama, USA*

<sup>22</sup>*Institute for Research in Schools, Canterbury, UK*

<sup>23</sup>*Department of Physics, Imperial College London, UK*

<sup>24</sup>*Centre for Astronomy, Astrophysics and Geophysics, Algiers, Algeria*

<sup>25</sup>*Department of Physics, University of British Columbia, Vancouver, British Columbia, Canada*

<sup>26</sup>*Formerly at Department of Physics and Applied Physics,  
Nanyang Technological University, Singapore – Associate member*

<sup>27</sup>*Department of Physics and Astronomy,  
Tufts University, Medford, Massachusetts, USA*

<sup>28</sup>*Physics Department, Northeastern University, Boston, Massachusetts, USA*

<sup>29</sup>*INFN, CNAF, Bologna, Italy*

<sup>30</sup>*Physics Department, Konkuk University, Seoul, Korea*

(Dated: December 27, 2017)

We update our previous search for trapped magnetic monopoles in LHC Run 2 using nearly six times more integrated luminosity and including additional models for the interpretation of the data. The MoEDAL forward trapping detector, comprising 222 kg of aluminium samples, was exposed to  $2.11 \text{ fb}^{-1}$  of 13 TeV proton-proton collisions near the LHCb interaction point and analysed by searching for induced persistent currents after passage through a superconducting magnetometer. Magnetic charges equal to the Dirac charge or above are excluded in all samples. The results are interpreted in Drell-Yan production models for monopoles with spins 0, 1/2 and 1: in addition to standard point-like couplings, we also consider couplings with momentum-dependent form factors. The search provides the best current laboratory constraints for monopoles with magnetic charges ranging from two to five times the Dirac charge.

PACS numbers: 14.80.Hv, 13.85.Rm, 29.20.db, 29.40.Cs

## I. INTRODUCTION

The magnetic monopole is motivated by the symmetry between electricity and magnetism, by grand-unification theories [1–4], and by the fundamental argument advanced by Dirac that its existence would explain why electric charge is quantised [5]. Dirac’s argument also predicts the minimum magnetic charge that a monopole should carry, the Dirac charge  $g_D$ , which is equivalent to 68.5 times the elementary electric charge, thus implying that a fast monopole should ionise matter at least a thousand times more than a proton or electron.

The initial Dirac monopole was assumed to be a point-like structureless source of magnetic poles, and as such its underlying microscopic theory is completely unknown. Monopoles with masses that could be in a range accessible to colliders have been predicted to exist within extensions of the standard model [6–10]. Other potentially low-mass monopoles within grand-unification theories or string-inspired models have also been predicted recently [11, 12]. However, these exhibit detailed structure and as a consequence their production by particle collisions is expected to be suppressed [13], although enhanced production might be expected in environments with strong magnetic fields and high temperatures, such as those characterising heavy ion collisions [14, 15]. In our searches, we adopt an open point of view and strive to probe direct monopole production beyond previous experimental constraints, without theoretical prejudice other than assuming a massive object carrying a multiple of the Dirac magnetic charge.

Direct searches for monopoles were performed each time a new energy regime was made available in a laboratory, including the CERN Large Electron-Positron (LEP) collider, the HERA electron-proton collider at DESY, and the Tevatron proton-antiproton collider at Fermilab, where direct pair production of monopoles was excluded up to masses of the order of 400 GeV for monopole charges in the range  $1g_D - 6g_D$  [16–19]. To cover the broadest possible ranges of masses, charges and cross sections, LHC-based direct searches for monopoles ought to use several complementary techniques, including general-purpose detectors, dedicated detectors, and trapping [20]. Searches were made in data samples of 7 and 8 TeV proton-proton ( $pp$ ) collisions at the LHC with the ATLAS and MoEDAL experiments, probing the TeV scale for the first time and excluding masses up to about 1 TeV [21–23]. As of 2015, masses up to 6 TeV can be probed in 13 TeV  $pp$  collisions. The first constraints made by direct measurement in this energy regime were set by an analysis of the MoEDAL forward trapping detector exposed to  $0.371 \text{ fb}^{-1}$  of  $pp$  collisions in 2015 [24], providing the best sensitivity to date in the range  $2g_D - 5g_D$ .

This paper presents a new search with the MoEDAL forward monopole trapping detector [24], using the same trapping array with both 2015 and 2016 exposures at LHC point-8. This corresponds to  $2.11 \pm 0.02 \text{ fb}^{-1}$  of 13 TeV  $pp$  collisions. The trapping volume consists of 672 square aluminium rods with dimension  $19 \times 2.5 \times 2.5 \text{ cm}^3$  for a total mass of 222 kg in 14 stacked boxes which were placed 1.62 m from the IP8 LHC interaction point under the beam pipe on the side opposite to the LHCb detector. The setup and conditions of exposure are identical to those used in the previous search [24].

---

\* Corresponding author:  
philippe.mermod@cern.ch

## II. MAGNETOMETER MEASUREMENTS

The 672 exposed aluminium samples of the MoEDAL forward trapping detector array were scanned in Spring 2017 during a two-week campaign with a DC SQUID long-core magnetometer (2G Enterprises Model 755) located at the laboratory for natural magnetism at ETH Zurich. Each sample was passed through the sensing coil at least once, with recordings of the magnetometer response in all three coordinates before, during, and after passage. The persistent current is defined as the difference between the measured responses in the  $z$  coordinate (along the shaft) after and before passage of the sample, to which the contribution of the conveyor tray is subtracted. A calibration factor obtained from special calibration runs using two independent methods [23–25] is used to translate this value into the measured magnetic charge in the samples in units of Dirac charge.

Persistent currents measured for all 672 samples for the first passage are shown in the top panel of Fig. 1. Samples for which this measurement significantly deviates from zero are set aside as candidates for further study. This method is based on the assumption of strong monopole binding in matter [26] and its great advantage is that the measurement can be repeated as many times as needed to minimise systematic errors and increase the sensitivity to the desired level. The threshold in the absolute value of the persistent current beyond which a sample is selected as a candidate is chosen here to be  $> 0.4g_D$  as a compromise between allowing sensitivity to magnetic charges down to  $1g_D$  and the time and effort required to scan a large number of samples multiple times. This gives 43 candidates, which were remeasured at least two more times each, as shown in the bottom panel of Fig. 1. These multiple measurements do not yield consistent non-zero persistent current values, confirming that all candidates identified in the first pass were false positives.

During this measurement campaign, the identification of false positives was dominated by two effects. The first effect, which was already observed in the previous runs [24], tends to happen with samples containing magnetic dipole impurities: whenever the sample magnetisation results in a flux inside the SQUID loop which temporarily exceeds the fundamental flux quantum  $\Phi_0 = \frac{h}{2e}$  [27] within a given margin, the response may not return to the same level during the flux change in the other direction, causing a slight offset. This is observed to happen with magnetised samples re-

gardless of exposure to LHC collisions. In this set of measurements, the offsets tend to take a value around  $\pm 1.8g_D$ . Measuring such samples multiple times will occasionally result again in an offset, faking the response of a monopole with charge  $\pm 1.8g_D$ . However, unlike a genuine monopole signature, it also occasionally yields zero; and turning the sample around such as to reverse its magnetisation in the  $z$  direction consistently reverses the sign of the offset. Similar systematic offsets could be reproduced in special runs with a calibration sample (magnetisation corresponding to  $10^4g_D$ ) and with rock samples (magnetisation corresponding to  $10^3g_D$ ). These tests confirm that the probability for an offset depends on the sample magnetisation. Moreover, it was determined that the offset value increases with increasing speed of transport through the sensing coils, supporting the hypothesis that it is related to trapped fluxes inside the SQUID that occur when the slew rate is increased.

The second effect is a slight deterioration of the  $z$  measurements due to random flux jumps occurring in the  $x$  and  $y$  measurements. Tests performed with aluminium samples and rock samples confirm that the jumps in  $x$  and  $y$  do not impact the reliability of the measurement in  $z$  besides resulting in small fluctuations which simply degrade the resolution. The instabilities in the  $x$  and  $y$  sensors were found to be related to two phenomena: 1) build up of static charge on the sample tray while it moved along the track and 2) capturing of stray fields in the magnetometer. To mitigate these effects, an anti-static brush was installed along the sample holder track before it enters the magnetometer; all cables between the SQUIDS and electronics were shielded; and the mu-metal shielding was grounded. Instrument performance is now improved and is expected to provide more stable results in future measurements.

Special care is given to the assessment of the probability for false negatives, i.e., the possibility that a monopole in a sample would remain unseen in the first pass due to a spurious fluctuation cancelling its response and resulting in a persistent current below the  $0.4g_D$  threshold used to identify candidates. This is studied using the distribution of persistent currents obtained in samples without monopoles (top panel of Fig 1), assuming that the magnetic field of the monopole itself (small compared to those of magnetic dipoles contained in the sample and tray) does not affect the mismeasurement probability. The distribution can be very well fitted using a sum of four Gaussians (two centred around zero, and two around  $\pm 1.8g_D$ ).

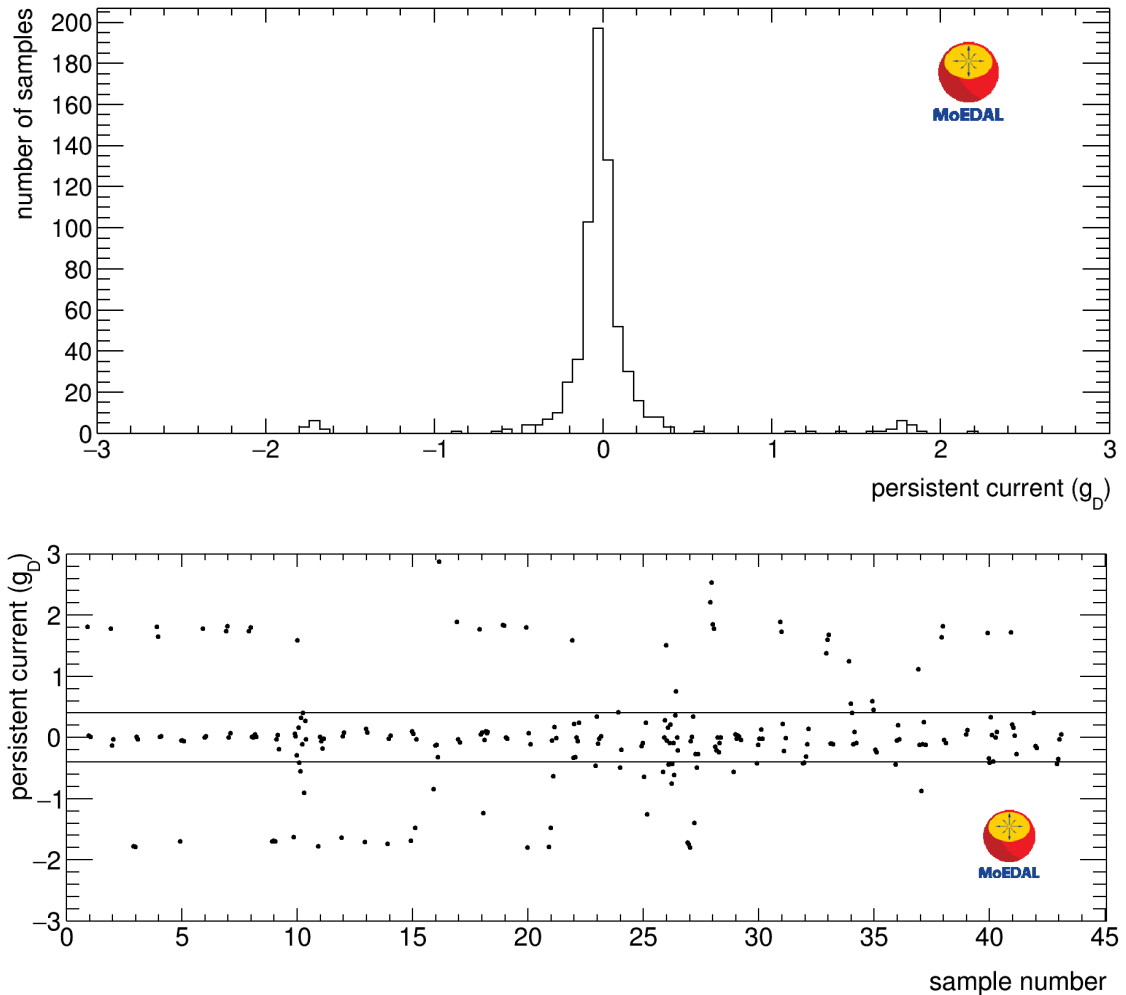


FIG. 1. Top: persistent current (in units of  $g_D$  after application of a calibration constant) after first passage through the magnetometer for all samples. Bottom: results of repeated measurements of candidate samples with absolute measured values in excess of  $0.4g_D$ .

The probability to miss a monopole is then estimated by integrating the fitted function in the relevant intervals: it is found to be less than 0.02% for a magnetic charge  $\pm 1g_D$ , less than 1.5% for a magnetic charge  $\pm 2g_D$ , and negligible for higher magnetic charges. These numbers could in principle be made even smaller by performing multiple measurements on all 629 non-candidate samples. However the level of detector efficiency obtained with the approach used is conservatively estimated to be 98%. This is considered adequate for the search being performed and this efficiency is assumed for the final interpretation.

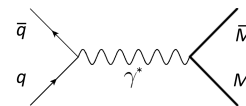


FIG. 2. Feynman diagrams for monopole pair production at leading order via the Drell-Yan process at the LHC. The non-perturbative nature of the process is ignored in the interpretation of the search.

### III. INTERPRETATION IN PAIR-PRODUCTION MODELS

The trapping detector acceptance, defined as the probability that a monopole of given mass, charge, energy and direction would end its tra-

jectory inside the trapping volume, is determined from the knowledge of the material traversed by the monopole [23] and the ionisation energy loss of monopoles when they go through matter [28–31] implemented in a simulation based on GEANT4 [32]. For a given mass and charge, the pair production model determines the kinematics and the overall trapping acceptance can be obtained. The uncertainty in the acceptance is dominated by uncertainties in the material description [23, 24]. This contribution is estimated by performing simulations with material conservatively added and removed from the geometry model.

A Drell-Yan (DY) mechanism (Fig. 2) is traditionally employed in searches to provide a simple model of monopole pair production [21–24]. In the interpretation of the present search, spin 1 is considered in addition to the spins 0 and 1/2 considered previously. The monopole magnetic moment is assumed to be zero and the coupling to the  $Z$  boson is neglected. Models were generated in MADGRAPH5 [33] using only tree level diagrams and the PDF NNPDF2.3 [34]. For comparison with previous studies, we also consider the possibility of a modification of the usual point-like QED coupling, where the monopole coupling  $g$  is substituted by  $\beta g$  with  $\beta = \frac{v}{c} = \sqrt{1 - \frac{4M^2}{s}}$  (where  $M$  is the mass of the monopole and  $\sqrt{s}$  is the invariant mass of the monopole-antimonopole pair). Such a modification, hereafter referred to as “ $\beta$ -dependent coupling”, has been advocated in some studies [26, 35–38], and has been used to interpret some previous monopole searches [17, 19, 21, 39], although it does not find unanimous support in the community. Nevertheless, using six different models for the interpretation of this search, with different angular and energy distributions, gives some measure how model uncertainties affect the search acceptance. The reliability of all these models is limited no matter how, as current theories cannot handle the non-perturbative regime of strong magnetic couplings.

The kinematic distributions of the various DY models generated by MADGRAPH are shown in Fig. 3. Differences are observed between the different spin assumptions due to kinematic constraints imposed by angular momentum conservation. A comparison of  $\beta$ -dependent and  $\beta$ -independent photon-monopole coupling models show similar pseudorapidity distributions and a higher monopole energy on average for the  $\beta$ -dependent coupling. This is expected because, in this case, the probability of generating a low-velocity monopole is suppressed by

a factor  $\beta < 1$ .

The behaviour of the acceptance as a function of mass has two contributions: the mass dependence of the kinematic distributions, and the velocity dependence of the energy loss (lower at lower velocity for monopoles). For monopoles with  $|g| = g_D$ , losses predominantly come from punching through the trapping volume, resulting in the acceptance showing U-shape with a minimum around 3000 GeV. The reverse is true for monopoles with  $|g| > g_D$  that predominantly stop in the upstream material and for which the acceptance is highest for intermediate masses. The acceptance reaches below 0.1% for a charge of  $6g_D$ , in which case the interpretation ceases to be meaningful because the systematic uncertainties become too large. The spin dependence is solely due to the different event kinematics.

Simulations with uniform monopole energy distributions allow identification, for various charge and mass combinations, of ranges of kinetic energy and polar angle for which the acceptance is relatively uniform, called fiducial regions. As the geometry of the setup used for this search is very similar to that of Ref. [23] although with a slightly thicker trapping detector array, the fiducial regions given in this reference can conservatively be used to provide an interpretation which does not depend on the monopole production model.

Cross-section limits for DY monopole production with the two coupling hypotheses ( $\beta$ -independent and  $\beta$ -dependent) and three spin hypotheses (0, 1/2, 1) are shown in Fig. 4. They are extracted from the knowledge of the acceptance estimates and their uncertainties; the integrated luminosity  $2.11 \pm 0.02 \text{ fb}^{-1}$  corresponding to 2015 and 2016 exposure to 13 TeV  $pp$  collisions; the expectation of strong binding to aluminium nuclei [26] of monopoles with velocity  $\beta \leq 10^{-3}$ ; and the non-observation of magnetic charge inside the trapping detector samples, with a 98% efficiency (see Section II).

Cross sections computed at leading order are shown as solid lines in Fig. 4, with the caveat that the coupling of the monopole to the photon is so large that perturbative calculations are not expected to be reliable. Using these cross sections and the limits set by the search, indicative mass limits are extracted and reported in Table I for magnetic charges up to  $5g_D$ . No mass limit is given for the spin-1/2  $5g_D$  monopole with standard point-like coupling, because in this case the low acceptance at small mass does not allow MoEDAL to exclude the full range down to the mass limit set at the Tevatron of around 400 GeV [17].

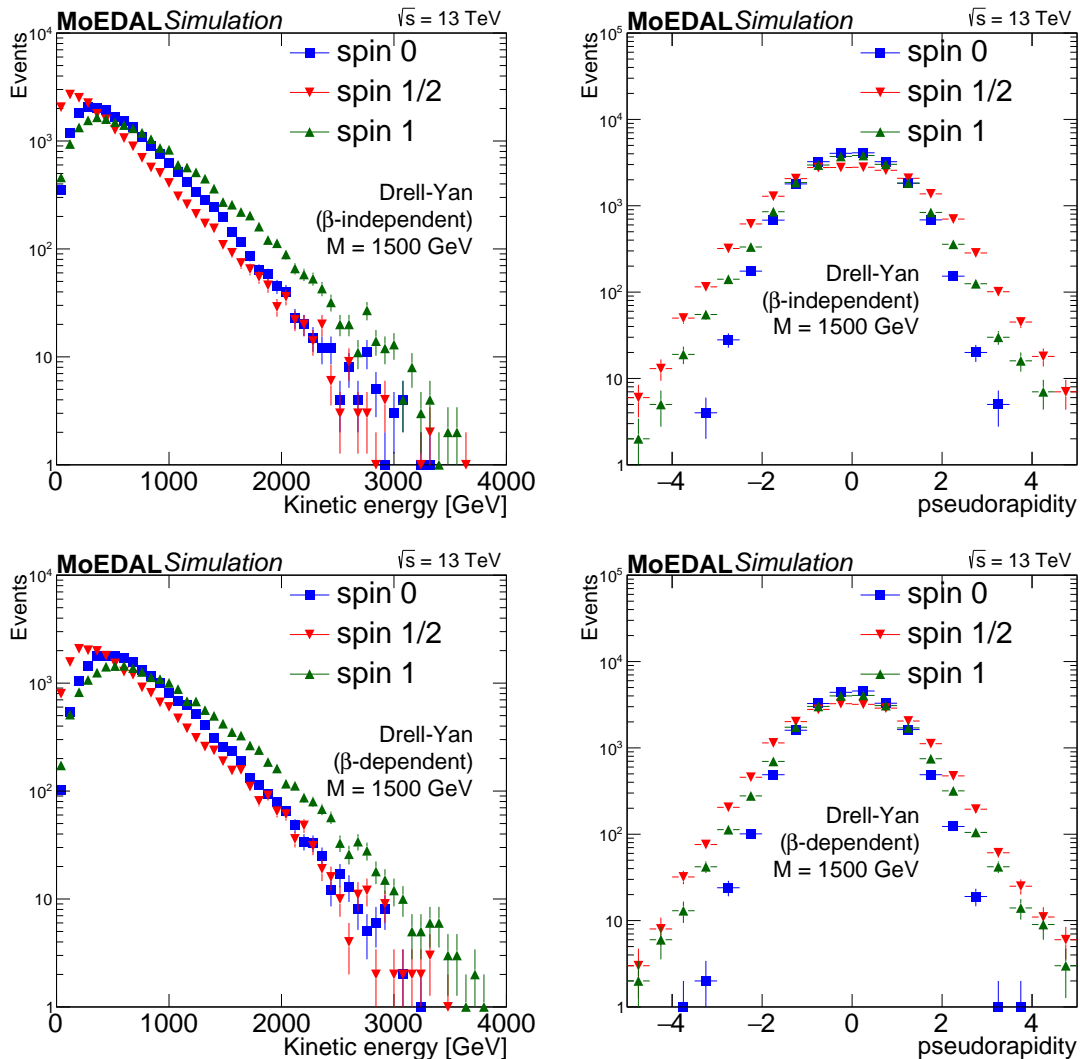


FIG. 3. Kinematic distributions of kinetic energy (left) and pseudorapidity (right) for monopoles with mass 1500 GeV for the standard (top) and  $\beta$ -dependent (bottom) photon-monopole couplings in models of Drell-Yan pair production generated by MADGRAPH. The three different monopole spin hypotheses (0, 1/2, 1) are superimposed.

#### IV. CONCLUSIONS

In summary, the aluminium elements of the MoEDAL trapping detector exposed to 13 TeV LHC collisions in 2015 and 2016 were scanned using a SQUID-based magnetometer to search for the presence of trapped magnetic charge. No genuine candidates were found. Consequently, monopole-pair direct production cross-section limits in the range 200 – 10000 fb were set for magnetic charges up to  $5g_D$  and masses up to 6 TeV. This translates in the strongest limits to date at a collider experiment [40] for charges ranging from two to five times the Dirac charge. For the first time, the possibility of

spin-1 monopoles was considered in addition to spin-0 and spin-1/2, using a Drell-Yan pair-production model.

#### ACKNOWLEDGEMENTS

We thank CERN for the very successful operation of the LHC, as well as the support staff from our institutions without whom MoEDAL could not be operated efficiently. We acknowledge the invaluable assistance of members of the LHCb Collaboration, in particular Guy Wilkinson, Rolf Lindner, Eric Thomas, and Gloria Corti. We

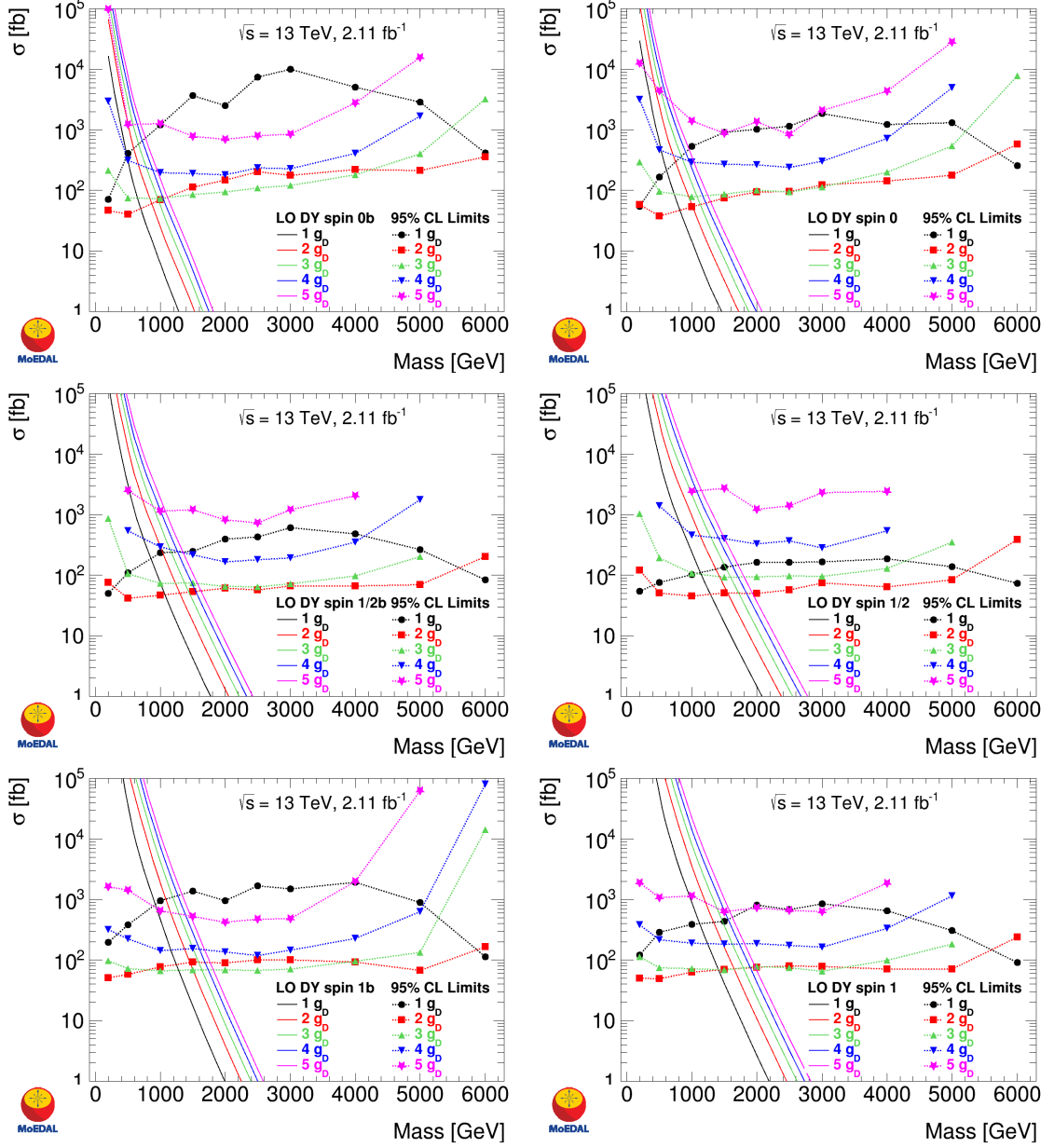


FIG. 4. Cross-section upper limits at 95% confidence level for the DY monopole pair production model Drell-Yan with  $\beta$ -dependent (left) and  $\beta$ -independent (right) couplings in 13 TeV  $pp$  collisions as a function of mass for spin-0 (top), spin-1/2 (middle) and spin-1 (bottom) monopoles. The colours correspond to different monopole charges. Acceptance loss is dominated by monopoles punching through the trapping volume for  $|g| = g_D$  while it is dominated by stopping in upstream material for higher charges, explaining the shape difference. The solid lines are cross-section calculations at leading order.

thank M. King, R. Staszewski and T. Whyntie for their help with the software. Computing support was provided by the GridPP Collaboration [41, 42], in particular from the Queen Mary University of London and Liverpool grid sites. This work was supported by grant PP00P2.150583 of the Swiss National Science Foundation; by the UK Science and Tech-

nology Facilities Council (STFC), via the research grants ST/L000326/1, ST/L00044X/1, ST/N00101X/1 and ST/P000258/1; by the Spanish Ministry of Economy and Competitiveness (MINECO), via the grants Grants No. FPA2014-53631-C2-1-P and FPA2015-65652-C4-1-R; by the Generalitat Valenciana via the special grant for MoEDAL CON.21.2017-

Mass limits [GeV]	$1g_D$	$2g_D$	$3g_D$	$4g_D$	$5g_D$
MoEDAL 13 TeV (2016 exposure)					
DY spin-0	600	1000	1080	950	690
DY spin- $\frac{1}{2}$	1110	1540	1600	1400	–
DY spin-1	1110	1640	1790	1710	1570
DY spin-0 $\beta$ -dep.	490	880	960	890	690
DY spin- $\frac{1}{2}$ $\beta$ -dep.	850	1300	1380	1250	1070
DY spin-1 $\beta$ -dep.	930	1450	1620	1600	1460
MoEDAL 13 TeV (2015 exposure)					
DY spin-0	460	760	800	650	–
DY spin- $\frac{1}{2}$	890	1250	1260	1100	–
MoEDAL 8 TeV					
DY spin-0	420	600	560	–	–
DY spin- $\frac{1}{2}$	700	920	840	–	–
ATLAS 8 TeV					
DY spin-0	1050	–	–	–	–
DY spin- $\frac{1}{2}$	1340	–	–	–	–

TABLE I. 95% confidence level lower mass limits in models of spin-0, spin-1/2 and spin-1 monopole pair production in LHC  $pp$  collisions. The present results (after 2016 exposure) are interpreted for Drell-Yan production with both beta-dependent and beta-independent couplings. These limits are based upon cross sections computed at leading order and are only indicative since the monopole coupling to the photon is too large to allow for perturbative calculations. Previous results obtained at the LHC are from Refs. [23, 24] (MoEDAL in previous exposures) and Ref. [22] (ATLAS).

09.02.03 and via the Projects PROMETEO-II/2014/066 and PROMETEO-II/2017/033; by the Spanish Ministry of Economy, Industry and Competitiveness (MINEICO), via the Grants No. FPA2014-53631-C2-1-P, FPA2014-54459-P, FPA2015-65652-C4-1-R and FPA2016-77177-C2-1-P; and by the Severo Ochoa Excellence Centre Project SEV-2014-0398; by the Physics Department of King's College London; by a Natural Science and Engineering Research Council of Canada via a project grant; by the V-P Research of the University of Alberta; by the Provost of the University of Alberta; by UEFISCDI (Romania); by the INFN (Italy); and by the Estonian Research Council via a Mobilitas Plus grant MOBTT5.

- 
- [1] G. 't Hooft, Nucl. Phys. B **79**, 276 (1974).  
[2] A. M. Polyakov, JETP Lett. **20**, 194 (1974).  
[3] D. M. Scott, Nucl. Phys. B **171**, 95 (1980).  
[4] J. Preskill, Ann. Rev. Nucl. Part. Sci. **34**, 461 (1984).  
[5] P. A. M. Dirac, Proc. Roy. Soc. **A 133**, 60 (1931).  
[6] Y. M. Cho and D. Maison, Phys. Lett. B **391**, 360 (1997), arXiv:hep-th/9601028 [hep-th].  
[7] K. Kimm, J. H. Yoon, and Y. M. Cho, Eur. Phys. J. C **75**, 67 (2015), arXiv:1305.1699 [hep-ph].  
[8] J. Ellis, N. E. Mavromatos, and T. You, Phys. Lett. B **756**, 29 (2016), arXiv:1602.01745 [hep-ph].  
[9] S. Arunasalam and A. Kobakhidze, Eur. Phys. J. C **77**, 444 (2017), arXiv:1702.04068 [hep-ph].  
[10] J. Ellis, N. E. Mavromatos, and T. You, Phys. Rev. Lett. **118**, 261802 (2017), arXiv:1703.08450 [hep-ph].  
[11] T. W. Kephart, G. K. Leontaris, and Q. Shafi, JHEP **10**, 176 (2017), arXiv:1707.08067 [hep-ph].  
[12] N. E. Mavromatos and S. Sarkar, Phys. Rev. D **95**, 104025 (2017), arXiv:1607.01315 [hep-th].  
[13] A. K. Drukier and S. Nussinov, Phys. Rev. Lett. **49**, 102 (1982).  
[14] O. Gould and A. Rajantie, Phys. Rev. D **96**, 076002 (2017), arXiv:1704.04801 [hep-th].  
[15] O. Gould and A. Rajantie, (2017), arXiv:1705.07052 [hep-ph].  
[16] OPAL Collaboration, Phys. Lett. B **663**, 37 (2008), arXiv:0707.0404 [hep-ex].  
[17] G. R. Kalbfleisch, W. Luo, K. A. Milton, E. H. Smith, and M. G. Strauss, Phys. Rev. D **69**, 052002 (2004), arXiv:hep-ex/0306045 [hep-ex].  
[18] H1 Collaboration, Eur. Phys. J. C **41**, 133 (2005), arXiv:hep-ex/0501039 [hep-ex].  
[19] CDF Collaboration, Phys. Rev. Lett. **96**, 201801 (2006), arXiv:hep-ex/0509015 [hep-ex].  
[20] A. De Roeck, A. Katre, P. Mermod, D. Milstead, and T. Sloan, Eur. Phys. J. C **72**, 1985 (2012), arXiv:1112.2999 [hep-ph].  
[21] ATLAS Collaboration, Phys. Rev. Lett. **109**, 261803 (2012), arXiv:1207.6411 [hep-ex].  
[22] ATLAS Collaboration, Phys. Rev. D **93**, 052009 (2016), arXiv:1509.08059 [hep-ex].  
[23] MoEDAL Collaboration, JHEP **08**, 067 (2016), arXiv:1604.06645 [hep-ex].  
[24] MoEDAL Collaboration (MoEDAL), Phys. Rev. Lett. **118**, 061801 (2017),



- arXiv:1611.06817 [hep-ex].
- [25] A. De Roeck, H.-P. Hächler, A. M. Hirt, M. Dam Joergensen, A. Katre, P. Mermod, D. Milstead, and T. Sloan, *Eur. Phys. J. C* **72**, 2212 (2012), arXiv:1206.6793 [physics.ins-det].
  - [26] K. Milton, *Rep. Prog. Phys.* **69**, 1637 (2006), arXiv:hep-ex/0602040 [hep-ex].
  - [27] This corresponds to  $66g_D$  for the  $z$  direction taking into account the transfer from the pick-up coil and the specifications of the magnetometer.
  - [28] S. P. Ahlen, *Phys. Rev. D* **17**, 229 (1978).
  - [29] S. P. Ahlen, *Rev. Mod. Phys.* **52**, 121 (1980).
  - [30] S. P. Ahlen and K. Kinoshita, *Phys. Rev. D* **26**, 2347 (1982).
  - [31] S. Cecchini, L. Patrizii, Z. Sahnoun, G. Sirri, and V. Togo, (2016), arXiv:1606.01220 [physics.ins-det].
  - [32] GEANT4 Collaboration, *IEEE Trans. Nucl. Sci.* **53**, 270 (2006).
  - [33] J. Allwall, M. Herquet, F. Maltoni, O. Matelaer, and T. Stelzer, *JHEP* **06**, 128 (2011), arXiv:1106.0522 [hep-ph].
  - [34] R. D. Ball *et al.*, *Nucl. Phys. B* **867**, 244 (2013), arXiv:1207.1303 [hep-ph].
  - [35] J. Schwinger, K. A. Milton, W.-Y. Tsai, L. L. DeRaad, and D. C. Clark, *Annals of Physics* **101**, 451 (1976).
  - [36] L. P. Gamberg, G. R. Kalbfleisch, and K. A. Milton, *Found. Phys.* **30**, 543 (2000).
  - [37] Yu. Kurochkin, I. Satsunkevich, D. Shoukavy, N. Rusakovich, and Yu. Kulchitsky, *Mod. Phys. Lett. A* **21**, 2873 (2006).
  - [38] L. N. Epele, H. Fanchiotti, C. A. Garcia Canal, V. A. Mitsou, and V. Vento, *Eur. Phys. J. Plus* **127**, 60 (2012), arXiv:1205.6120 [hep-ph].
  - [39] G. R. Kalbfleisch, K. A. Milton, M. G. Strauss, L. Gamberg, E. H. Smith, and W. Luo, *Phys. Rev. Lett.* **85**, 5292 (2000), arXiv:hep-ex/0005005 [hep-ex].
  - [40] C. Patrignani *et al.* (Particle Data Group), *Chin. Phys. C* **40**, 100001 (2016).
  - [41] GridPP Collaboration, *J. Phys. G* **32**, N1 (2006).
  - [42] D. Britton *et al.*, *Phil. Trans. R. Soc. A* **367**, 2447 (2009).